PGC-1α plays a pivotal role in simvastatin-induced exercise impairment in mice

Miljenko Valentin Panajatovic[1,2], **François Singh**[1,2], **Noëmi Johanna Roos**[1,2], **Urs Duthaler**[1,2], **Christoph Handschin**[3], **Stephan Krähenbühl**[1,2,4], **Jamal Bouitbir**[*,1,2,4]

[1]Division of Clinical Pharmacology & Toxicology, University Hospital, Basel, Switzerland
[2]Department of Biomedicine, University of Basel, Switzerland [3]Biocenter, University of Basel, Basel, Switzerland [4]Swiss Centre for Applied Human Toxicology (SCAHT), Basel, Switzerland

Abstract

Aim—Statins decrease cardiovascular complications, but can induce myopathy. Here, we explored the implication of PGC-1α in statin-associated myotoxicity.

Methods—We treated PGC-1α knockout (KO), PGC-1α over-expression (OE) and wild-type mice (WT) mice orally with 5 mg simvastatin kg^{-1} day^{-1} for 3 weeks and assessed muscle function and metabolism.

Results—In WT and KO mice, but not in OE mice, simvastatin decreased grip strength, maximal running distance and vertical power assessed by ergometry. Post exercise plasma lactate concentrations were higher in WT and KO compared to OE mice. In glycolytic gastrocnemius, simvastatin decreased mitochondrial respiration, increased mitochondrial ROS production and free radical leak in WT and KO, but not in OE mice. Simvastatin increased mRNA expression of *Sod1*

[*]**Corresponding author:** Jamal Bouitbir, PhD, Clinical Pharmacology & Toxicology, University Hospital, 4031 Basel, Switzerland, Phone: +41 61 265 2395, Fax: +41 61 265 5401, jamal.bouitbir@unibas.ch.
DR JAMAL BOUITBIR (Orcid ID : 0000-0003-4453-9457)

Reprint request
Unfortunately, due to copyright-relatedt issues, we are not able to post the post-print pdf version of our manuscript - in some cases, not even any version of our manuscript. Thus, if you would like to request a post-production, publisher pdf reprint, please click send an email with the request to christoph-dot-handschin_at_unibas-dot-ch (see http://www.biozentrum.unibas.ch/handschin).
Information about the Open Access policy of different publishers/journals can be found on the SHERPA/ROMEO webpage: http://www.sherpa.ac.uk/romeo/

Reprint Anfragen
Aufgrund fehlender Copyright-Rechte ist es leider nicht möglich, dieses Manuskript in der finalen Version, z.T. sogar in irgendeiner Form frei zugänglich zu machen. Anfragen für Reprints per Email an christoph-dot-handschin_at_unibas-dot-ch (s. http://www.biozentrum.unibas.ch/handschin).
Informationen zur Open Access Handhabung verschiedener Verlage/Journals sind auf der SHERPA/ROMEO Webpage verfügbar: http://www.sherpa.ac.uk/romeo/

Conflict of interest:
The authors declare no competing financial interests. No potential conflicts of interest relevant to this article were reported.

Author contribution:
M.V.P., F.S., C.H., S.K. and B.J. conceived and designed study, and M.V.P., F.S., U.D., N.J.R., and B.J. performed experiments and analyzed data. M.V.P., S.K. and J.B. wrote the manuscript.

and *Sod2* in glycolytic and oxidative gastrocnemius of WT, but decreased it in KO mice. OE mice had a higher mitochondrial DNA content in both gastrocnemius than WT or KO mice and simvastatin exhibited a trend to decrease the citrate synthase activity in white and red gastrocnemius in all treatment groups. Simvastatin showed a trend to decrease the mitochondrial volume fraction in both muscle types of all treatment groups. Mitochondria were smaller in WT and KO compared to OE mice and simvastatin further reduced the mitochondrial size in WT and KO mice, but not in OE mice.

Conclusions—Simvastatin impairs skeletal muscle function, muscle oxidative metabolism and mitochondrial morphology preferentially in WT and KO mice, whereas OE mice appear to be protected, suggesting a role of PGC-1α in preventing simvastatin-associated myotoxicity.

Keywords

statins; PGC-1α; grip strength; exercise capacity; mitochondria; Reactive Oxygen Species (ROS)

1 Introduction

Statins (3-hydroxy-3-methylglutaryl coenzyme A reductase inhibitors) are effective low density lipoprotein (LDL)-cholesterol lowering drugs and belong to the most often prescribed medications in developed countries [1]. They reduce hepatic cholesterol synthesis by inhibiting the synthesis of mevalonate, the rate-limiting step in the cholesterol biosynthetic pathway [2]. Although the clinical benefits of statins in LDL-cholesterol lowering are well established, patients may suffer from muscle toxicity (termed statin-associated muscle symptoms, SAMS) [3], which affects up to 1 in 4 patients treated with statins. The clinical severity of SAMS ranges from asymptomatic elevation of creatine kinase (CK) activity to fatal rhabdomyolysis.

Our knowledge about the mechanisms of statin induced skeletal muscle injury is currently incomplete [4]. Several studies have suggested that mitochondria may play a role in statin-induced myotoxicity. By inhibiting the synthesis of mevalonate, statins impair the production of coenzyme Q, which is an important constituent of the electron transport chain [5]. Coenzyme Q deficiency may therefore be a cause for mitochondrial toxicity of statins, but its contribution to myotoxicity of statins is debated [4,6]. In addition, several studies have shown that statins can inhibit the function of the electron transport chain directly by inhibiting the function of enzyme complexes of the electron transport [3,7–9]. Mitochondria not only produce energy in the form of ATP, but are also important generators of reactive oxygen species (ROS), which can act either as a second messenger or as a source of cellular damage, depending on the amount ROS being produced [10–13]. In support of a role of mitochondrial ROS for statin-induced myopathy, we have shown in a previous study that treatment of rats with atorvastatin impaired the activity of enzyme complexes of the electron transport chain, increased skeletal muscle ROS and decreased exercise capacity [9].

The peroxisome proliferator-activated receptor gamma co-activator (PGC-1α) is a major regulator of mitochondrial biogenesis and represents a potential target for the effects of statins on skeletal muscle [14]. In support of this assumption, we have shown previously that statins impair mitochondrial biogenesis in skeletal muscle of both patients suffering from

SAMS as well as in rats [15]. Since over-expression of PGC-1α increases number and function of mitochondria in skeletal muscle [16] as well as the number of type IIa and type I oxidative slow twitch high endurance muscle fibers and endurance performance [17], PGC-1α over-expression may be able to prevent statin-associated myotoxicity. In contrast, statin-associated myotoxicity may be more accentuated in mice lacking PGC-1α.

Based on these considerations, we hypothesize that statins should decrease the physical performance of mice through skeletal muscle mitochondrial impairment, and that over-expression of PGC-1α should prevent, whereas PGC-1α knock-out should increase statin-induced myotoxicity compared to wild type mice. In the current study, we therefore investigated the effect of simvastatin on skeletal muscle function and muscle energy metabolism in wild-type mice (WT), PGC-1α muscle knock-out mice (KO mice) and in mice over-expressing PGC-1α (OE mice). Control mice for each group were treated with vehicle (water).

2   Results

2.1   Simvastatin treatment did not change physiological parameters

In order to assess possible changes in the overall physical condition of the mice, each mouse was monitored for body weight as well as food and water intake during the entire three weeks of treatment with either simvastatin or water (Table 1). After 3 weeks, a daily oral dose of 5 mg x kg^{-1} simvastatin did not affect the parameters mentioned above. The heart weight and the weight of the gastrocnemius and extensor digitorum longus (EDL) muscles were also not affected by the treatment with simvastatin. However, in WT mice, treatment with simvastatin was associated with an increase in the weight of the soleus muscle (Table 1). PGC-1α knockout or over-expression influenced the muscle weight only slightly. OE mice treated with water had a higher weight of the soleus muscle and a lower weight of quadriceps muscle compared to the respective WT mice.

2.2   Plasma concentration of simvastatin was similar in WT, PGC-1αKO and OE mice

Exposure to simvastatin in mice was analyzed in plasma by LC-MS/MS. As expected, we did not detect any simvastatin in plasma from mice treated with water. In mice treated with simvastatin, there was no significant difference between WT (average 14.7, range 9.68 – 21.3 nM), KO (average 7.11, range 3.78 – 11.7 nM), and OE mice (average 7.05, range 1.88 – 13.4 nM). The plasma concentrations were comparable to values measured in patients [18].

2.3   Simvastatin treatment decreased grip strength in WT and PGC-1αKO mice, but not in PGC-1αOE mice

To monitor mouse physical strength, we measured their grip strength once a week during the three weeks of treatment. Each grip strength was normalized to body weight at the day of grip strength measurement. Grip strength measurements obtained during treatment were compared to the initial grip strength at day 1 (set to 100% for control WT mice). Control mice in the WT, KO and OE groups showed stable grip strength over time, while mice treated with simvastatin showed a gradual decrease, which reached statistical significance at

day 22 in WT mice (Figure 1A) and KO mice (Figure 1B). Simvastatin did not affect the grip strength in OE mice (Figure 1C).

2.4 Simvastatin treatment decreased physical capacity in WT and PGC-1αKO mice, but not in PGC-1αOE mice

To evaluate muscle endurance, mice were stimulated to run on a treadmill until exhaustion (Figure 2A). In comparison to WT mice, KO mice ran a significantly shorter and OE mice a longer distance. Simvastatin decreased the running distance in WT and KO mice in comparison to their respective control mice, but showed no effect in OE mice (Figure 2A). Based on these data, we calculated the vertical mechanical power of the mice exerted during exercise (Figure 2B). In comparison to WT mice, KO mice developed less and OE mice more vertical power. We found no difference between simvastatin-treated and control mice in both WT and OE mice. However, simvastatin decreased vertical power exerted by KO mice (Figure 2B).

To further explain the differences in running distance between mice, we measured their plasma lactate concentration before and after exercise. Before exercise, lactate concentrations were similar in all groups (Figures 2C - 2E). Exercise increased the plasma lactate concentrations in all groups, but this increase was clearly lower in OE mice than in WT or KO mice. WT mice treated with simvastatin had a significantly higher post-exercise plasma lactate concentration than the respective control mice (Figure 2C). In the other groups, simvastatin did not affect the post-exercise plasma lactate concentration (Figures 2D and 2E).

To better understand the plasma lactate levels in mice after exercise, we checked the mRNA expression of the lactate transporters *Mct1* and *Mct4* involved in lactate import and export, respectively, in skeletal muscle. We observed mouse model effects on the mRNA expression on both *Mct1* and *Mct4* transporters in OE mice, with *Mct1* being upregulated (Suppl. Figure 1A) and *Mct4* downregulated (Suppl. Figure 1B) in glycolytic gastrocnemius. These data support the notion that the low lactate plasma levels in OE mice were not only due to a lower production in skeletal muscle, but also due to increased lactate reuptake from the blood.

Electrical shocks, which stimulated the mice to run, were measured during exercise on the treadmill. Simvastatin treated mice from both WT and KO groups displayed a curve shifted to the left in comparison to their respective control mice (Suppl. Figures 2A and 2B), which correlated with the shorter running distance. In comparison, treatment with simvastatin did not affect the number of shocks in OE mice (Suppl. Figure 2C). In order to analyze these graphs further, we calculated the time for the mice to reach 40 cumulative shocks. KO mice reached the 40 shocks threshold earlier in contrast to WT mice (Suppl. Figure 2D). In comparison, simvastatin significantly decreased the time for the mice to reach 40 shocks in KO mice, but led only to a numerical decrease in WT and OE mice (Suppl. Figure 2D). No differences were observed between control and simvastatin-treated OE mice.

2.5   Simvastatin did not change the metabolic respiratory measurements during exercise

We also examined O_2 consumption (VO_2) and CO_2 production (VCO_2) by the mice during exercise, as these parameters can serve as indicators for substrate utilization during exercise (Suppl. Figures 3A and 3B). We then calculated the respiratory exchange ratio (RER), which indicates preference for fatty acids when close to 0.7 and preference for glucose as substrate when close to 1. OE mice had an RER between 0.8 and 0.9 over the entire exercise period irrespective of treatment with simvastatin, indicating a preference for fatty acids as a fuel. In comparison, the RER of KO and WT mice were between 0.9 and 1.1, indicating a preference for glucose (Suppl. Figure 3C). As shown in Suppl. Table 1, the averaged RER at different time points confirm that the RER in OE mice were lower compared to KO and WT mice and they show that simvastatin did not significantly affect the RER. These findings correlate well the plasma lactate concentrations, which were lower in OE mice compared to WT and KO mice (Figures 2C-2E).

2.6   PGC-1α over-expression protected impairments of mitochondrial respiration produced by simvastatin in glycolytic and oxidative skeletal muscles

As a next step, we evaluated the mitochondrial function of the glycolytic gastrocnemius and of the oxidative soleus muscles. In both muscles, oxidation rates were higher for OE mice than for WT or KO mice (Figure 3). In the glycolytic gastrocnemius muscle, simvastatin decreased the maximal respiratory rates for complex I + II linked substrates in WT mice (Figure 3A) and for complex I linked respiration in KO mice (Figure 3B). In contrast, simvastatin did not affect the respiration of the gastrocnemius muscle from OE mice (Figure 3C). In the oxidative soleus muscle, mitochondrial respiration was not affected by simvastatin in WT mice (Figure 3D), but decreased complex I+II and complex II linked substrate respiration in soleus muscle from KO mice (Figure 3E). In the soleus muscle of OE mice, simvastatin did not significantly affect mitochondrial respiration (Figure 3F).

2.7   PGC-1α over-expression abolished the increase of mitochondrial H_2O_2 production and free radical leak produced by simvastatin in glycolytic skeletal muscles

As elevated mitochondrial H_2O_2 production can be deleterious to mitochondrial function [19], we next assayed this in our mice. Under reverse electron flux conditions, simvastatin increased mitochondrial H_2O_2 production in glycolytic white gastrocnemius, but not in soleus of WT mice (Figure 4A). In KO mice, H_2O_2 production was already at a high level in both treatment groups in white gastrocnemius in comparison to the respective WT mice and simvastatin did not further increase H_2O_2 production (Figure 4B). Similarly, simvastatin did not affect H_2O_2 production in OE mice (Figure 4C). We also calculated the free radical leak (FRL) by relating H_2O_2 production to mitochondrial respiration. As expected, the FRL was lowest for both soleus and gastrocnemius in OE mice and highest in KO mice (Figures 4D, 4E and 4F). Similar to H_2O_2 production, simvastatin increased the FRL only in gastrocnemius of WT mice (Figure 4D).

2.8   PGC-1α protected skeletal muscle from simvastatin-induced oxidative stress

A long-term increase in mitochondrial production of ROS can induce the antioxidative defense system. For that, we measured the mRNA expression of *Sod1* located in the cytosol

and the mitochondrial intermembrane space and of *Sod2* located in the mitochondrial matrix [20]. In glycolytic and oxidative parts of gastrocnemius muscle, *Sod1* mRNA expression increased in WT mice treated with simvastatin (Figures 5A and 5B). In KO mice, simvastatin decreased *Sod1* mRNA expression in both muscles (Figures 5A and 5B). In OE mice, simvastatin increased *Sod1* mRNA expression in the oxidative part of gastrocnemius muscle (Figure 5B), but had no significant effect in the glycolytic gastrocnemius (Figure 5A). SOD2 degrades superoxide anion and can be upregulated under conditions of increased mitochondrial ROS production [21]. Simvastatin treatment increased the *Sod2* mRNA expression in white and red gastrocnemius in WT mice (Figures 5C and 5D). However, in KO mice, simvastatin decreased *Sod2* mRNA expression in both muscle types (Figures 5C and 5D). In OE mice, *Sod2* mRNA expression was 2 to 3 times higher than in WT or KO mice, but was not affected by simvastatin in both muscle types (Figures 5C and 5D).

H_2O_2 generated by superoxide dismutation can be degraded to water by glutathione peroxidase in a reaction using glutathione. For this reason, we measured the glutathione pool in both gastrocnemius muscle types (Figures 5E and 5F). In WT mice, simvastatin did not affect the glutathione pool in glycolytic gastrocnemius muscle, but decreased it significantly in oxidative gastrocnemius. In comparison to WT mice, the glutathione pool in white gastrocnemius was significantly lower in KO mice (Figure 5E). However, simvastatin did not alter the glutathione pool in KO mice (Figure 5E). In OE mice, simvastatin treatment did not change the glutathione pool in the glycolytic and oxidative the gastrocnemius (Figures 5E and 5F).

2.9 Simvastatin did not affect citrate synthase activity in skeletal muscles

We measured citrate synthase activity (CS) and the mtDNA content as markers of mitochondrial content [22]. As expected, both citrate synthase activity and the mtDNA content normalized to muscle weight were higher in OE control compared to WT mice (in red gastrocnemius, the increase in citrate synthase activity was only numerical) (Figures 6A-6D). In comparison, citrate synthase activity was numerically lower in KO control compared to WT control mice, but without reaching statistical significance (Figures 6C and 6D). Simvastatin did not significantly affect citrate synthase activity and mtDNA content in white and red gastrocnemius, independently of PGC-1α expression.

2.10 Simvastatin induced changes in the mitochondrial cross area distribution

In order to investigate mitochondrial number and cross section distribution, we performed an electron microscopy analysis of the glycolytic and oxidative quadriceps muscle. In the glycolytic quadriceps muscle, the number of mitochondria was higher in OE as compared to WT and KO mice (Suppl. Figure 4A). In the glycolytic quadriceps muscle, simvastatin did not affect the number of mitochondria (Suppl. Figure 4A). In the oxidative quadriceps, the number of mitochondria was lower in KO compared to WT mice and there was no difference between WT and OE mice (Suppl. Figure 4B). In oxidative quadriceps muscle, simvastatin decreased the number of mitochondria in WT, but not in KO or OE mice (Suppl. Figure 4B).

Next, we evaluated the cross-sectional area of the individual mitochondria in each micrograph (Figure 7). Compared to WT or KO control mice, OE control mice had a larger

median cross-sectional area (0.30 μm^2 for both glycolytic and oxidative skeletal muscle; Figures 7D and 7H) as compared to KO (0.09 μm^2 and 0.14 μm^2 in glycolytic and oxidative muscle, respectively; Figures 7C and 7G) and WT mice (0.15 μm^2 and 0.13 μm^2 in glycolytic and oxidative muscle, respectively; Figures 7B and 7F). In WT mice, simvastatin decreased the median mitochondrial cross-sectional area in both glycolytic (from 0.15 μm^2 to 0.08 μm^2; Figure 7B) and in oxidative quadriceps muscle (from 0.13 μm^2 to 0.09 μm^2; Figure 7F). In KO mice, treatment with simvastatin had no relevant effect on the mitochondrial cross-sectional area in glycolytic quadriceps (0.15 μm^2 and 0.13 μm^2 in control and simvastatin-treated mice, respectively; Figure 7C), whereas it decreased the cross-sectional area in oxidative quadriceps (0.14 μm^2 and 0.11 μm^2 in control and simvastatin-treated mice, respectively; Figure 7G). In OE mice, simvastatin had no relevant effect on the mitochondrial cross-sectional area in glycolytic quadriceps (0.30 μm^2 and 0.29 μm^2 in control and simvastatin-treated mice, respectively; Figure 7D), whereas it increased the cross-sectional area in oxidative quadriceps from 0.30 μm^2 to 0.49 μm^2 (Figure 7H).

3 Discussion

The principle goal of this study was to investigate the effect of simvastatin on myotoxicity of mice with different skeletal muscle expression of PGC-1α. The hypothesis was that a high expression of PGC-1α would attenuate myotoxicity associated with simvastatin. Indeed, three weeks of treatment with simvastatin impaired skeletal muscle function and metabolism mainly in WT and PGC-1α KO mice, whereas PGC-1α OE mice were mostly unaffected. The study therefore supports the hypothesis that PGC-1α has a protective role in simvastatin-induced myotoxicity. We treated mice with an oral simvastatin dose of 5 mg/kg/day for three weeks, which should lead to similar exposures as observed in humans [18]. The dose was calculated as described by Reagan-Shaw et al. [23] and corresponds to approximately to 0.4 mg/kg/day in humans, which is a dose in the middle range used in humans. We have used the same dose in previous studies, in which we observed effects of simvastatin on skeletal muscle and heart metabolism [24,25]. The peak plasma concentrations in mice determined in the current study (ranging from 1.88 to 21.3 nM) were lower than those reported in patients treated with 40 mg simvastatin/day, who have peak concentrations in the range of 19-31 nM [18]. Importantly, we did not observe significant differences in the exposure to simvastatin among the treatment groups, indicating that the groups are comparable. *In vitro* toxicity in mouse skeletal muscle myotubes (C$_2$C$_{12}$ myotubes) typically starts at about 10 μM [25,26], which is higher than the peak concentrations in mice. It has to be taken into account, however, that the concentrations reached in muscle may be higher than in plasma and that immortalized cell lines may be less sensitive to statins than myocytes *in vivo*.

We showed that treatment with simvastatin for three weeks at 5 mg/kg/day decreased grip strength and exercise capacity in wild-type and in PGC-1α KO mice, but not in PGC-1α OE mice. In agreement with the current study, we reported in a previous publication that treatment of rats with atorvastatin at 10 mg/kg/day for two weeks decreased exercise capacity [9] and treatment of mice with atorvastatin at 5 mg/kg/day for two weeks decreased mice strength assayed by the grip test [27]. These findings confirm that the skeletal muscle of rodents is sensitive to statins. In the current study, simvastatin not only decreased the

running distance in WT and PGC-1α KO mice, but also increased the post-exercise plasma lactate concentration compared to the respective control mice. This suggested a switch from mitochondrial generation of ATP to glycolysis; an interpretation, which was supported by the observation that simvastatin increased the RER only in WT and PGC-1α KO mice, but not in PGC-1α OE mice. The reason for the switch from mitochondrial ATP generation to glycolysis may be a decrease in mitochondrial function by simvastatin, as shown in the current but also in previous studies [3,7,27–29]. In the current study, we found decreases in the activity of complex I and II-linked substrates, which is compatible with an impaired activity of complex I and II or also of complex III. A decrease in complex III activity by simvastatin has been described by Schirris et al. [3]. An impaired activity the electron transport chain, in particular of complex I or III, is a well-established reason for mitochondrial production of reactive oxygen species (ROS) [30]. Indeed, in the current study, we observed an increase in mitochondrial production of H_2O_2 in white gastrocnemius of WT but not of PGC-1α KO or PGC-1α OE mice. Increased mitochondrial production of ROS in association with statins has been described in previous studies [15,27,28,31]. Since the antioxidative capacity is lower in white than in red muscle [31], the finding that only the white gastrocnemius was affected, is not surprising. H_2O_2 production was not increased by simvastatin in PGC-1α KO mice, possibly because the production was already high in the absence of simvastatin. In comparison, the H_2O_2 production by white gastrocnemius muscle fibers from PGC-1α OE mice was low and not increased by simvastatin, suggesting that PGC-1α overexpression was protective. The protection against mitochondrial ROS in PGC-1α OE mice may have been mainly due to *Sod2*, which had a clearly higher expression in red and white gastrocnemius compared to WT and PGC-1α KO mice. Importantly, an increased intramitochondrial ROS concentration can impair the function of the enzyme complexes located in the inner mitochondrial membrane, in particular of complex I, III and IV, due to peroxidation of cardiolipin. Cardiolipin is important for the embedment of these enzyme complexes in the inner mitochondrial membrane and also for their function [32]. This mechanism could explain the impairment of the function of the mitochondrial electron transport chain by statins.

PGC-1α is an inducible co-regulator of nuclear transcription factors that are involved mainly in energy metabolism [33]. As confirmed by the current study, mice with whole body [34] or muscle-specific [16] knock-out of PGC-1α showed a reduced exercise capacity. In comparison, mice with a muscle specific over-expression of PGC-1α had an increased exercise capacity [35]. The improvement of skeletal muscle performance in mice with muscular overexpression of PGC-1α can be explained by an increase in the mitochondrial volume fraction and mitochondrial function as well as by a shift from glycolytic to oxidative muscle fibers [16]. In agreement with these previous observations, we detected an increase in the activity of the enzyme complexes of the electron transport chain mainly in white (glycolytic), but also in red (oxidative) muscle fibers from PGC-1α OE mice. An obvious explanation for these findings is the increase in the mitochondrial copy number and volume fraction that we observed in the glycolytic and oxidative muscle of PGC-1α OE mice. We have shown in a previous study that atorvastatin can induce a shift from an oxidative to a glycolytic fiber type in skeletal muscle of mice [27]. We considered this fiber shift to be one of the reasons for statin-induced myotoxicity, since glycolytic fibers have less antioxidative capacity and are more vulnerable to statins [4,26]. On the other hand, as stated above, muscle-

specific overexpression of PGC-1α in mice leads to a shift from glycolytic to oxidative fibers [30,36]. Since statins exert their myotoxicity at least partially via increased mitochondrial production of ROS [15,28,31], this switch from glycolytic to oxidative muscle fibers could possibly explain the protection of PGC-1α OE mice from simvastatin-associated myotoxicity observed in the current study.

Interestingly, PGC-1α OE mice not only had more, but also larger mitochondria. While simvastatin decreased the size of mitochondria in WT and PGC-1α KO mice, this was not the case in PGC-1α OE mice. The decrease in mitochondrial size in WT and PGC-1α KO mice may represent mitochondrial fission, which may be a consequence of mitochondrial toxicity of simvastatin. If mitochondrial toxicity by statins is mainly due to increased production of ROS [15,28,31], mitochondria in PGC-1α OE mice may be protected by the observed increase in *Sod2* mRNA expression levels. This increase appears to be more accentuated than the increase in the mitochondrial DNA content or volume fraction, suggesting that PGC-1α overexpression not only stimulates mitochondrial biogenesis, but may also affect certain aspects of mitochondrial function. In conclusion, treatment with simvastatin reduced grip strength and exercise performance in WT and PGC-1α KO mice, whereas PGC-1α OE mice were protected. Simvastatin increased ROS production in the glycolytic muscle of WT mice, but not of PGC-1α OE mice, which may have been protected by a high expression of *Sod2*. Simvastatin impaired the function of enzyme complexes of the mitochondrial electron transport chain in WT and PGC-1α KO mice, but not in PGC-1α OE mice. Muscular overexpression of PGC-1α protected mice from simvastatin-induced myotoxicity by a switch from glycolytic to oxidative muscle fibers, which have a higher mitochondrial content and antioxidative capacity.

4 Materials and methods

4.1 Animals

The three mouse models used for the purpose of the study include the PGC-1α muscle knockout mice (KO), mice with skeletal muscle PGC-1α overexpression (OE) and wild-type mice (WT). These breeding pairs of these mouse models were kindly provided by Prof. Handschin (University of Basel, Switzerland). Generation of knockout (KO) mice using the Cre/LoxP system by „floxing" *Ppargc1a* allele has been described previously [36]. Breeding was performed by crossing female floxed *Ppargc1a* allele homozygote mice expressing Cre recombinase with male floxed *Ppargc1a* homozygote which did not express Cre recombinase. Cre recombinase was selectively expressed in muscle tissues due to its position at the DNA level under the control of the myogenin promoter and MEF2C enhancer [37]. PGC-1α overexpressing mice with myogenin promotor sequence were generated using the DNA microinjection technique. These mice have *Ppargc1a* expression under the control of the muscle creatine kinase promotor preferentially expressed in type II fibers [35]. Wild type (WT) mice used in experiments included mice with floxed *Ppargc1a* allele homozygotes which did not express Cre recombinase and OE mice which did not overexpress the *Ppargc1a* gene.

4.2   Study design and simvastatin administration

Experiments were performed on adult mice (15-17 weeks at the beginning of the study). Animals were housed in neutral temperature environment (22° ± 2 °C) on a 12:12 hour photoperiod and had free access to food and water. All experiments were performed in agreement with the guidelines from Directive 2010/63/EU of the European Parliament on the protection of animals used for scientific purposes. Experiments were reviewed and accepted by the cantonal veterinary authority of Basel and were performed in agreement with the guidelines for care and use of laboratory animals (License 2847).

After one week of acclimatization, mice of each model were randomly divided in 6 groups as follows: (1) WT treated with water (Ctl, n=10); (2) WT treated with simvastatin 5 mg/kg/day (Simv, n=10); (3) KO mice treated with water (n=10); (4) KO mice treated with simvastatin 5 mg/kg/day (n=10), (5) OE mice treated with water (n=10); and (6) OE mice treated with simvastatin 5 mg/kg/day (n=10). These mice were treated by oral gavage for three weeks [26]. Body weight, food and water intake were measured daily during the treatment period.

4.3   Simvastatin concentration in plasma

For the measurement of simvastatin in mouse plasma, we treated 4 mice per group one hour before the sacrifice. The one-hour time point was selected based on the corresponding maximum concentration (T_{max}) [38]. Simvastatin acid was analysed in mouse plasma by high-pressure liquid chromatography tandem mass spectrometry (HPLC-MS/MS). A HPLC system from Shimadzu (Kyoto, Japan) which was connected to a triple quadrupole mass spectrometer from AB Sciex (API 4000 Qtrap, Concord, Canada) was used for the measurements. Calibration lines of simvastatin acid were prepared in drug free mouse plasma from 0.5 nM (lower limit of quantification (LLOQ)) to 200 nM. Unknown samples were quantified based on linear regressions of known simvastatin acid concentration (x) and the peak area ratio of simvastatin to simvastatin acid-d6 (y). Regressions were weighted by $1/x2$. Aliquots of 10 μL plasma were extracted with 200 μL methanol containing 100 nM simvastatin acid-d6 (internal standard (IS)). Samples were thoroughly vortex mixed and centrifuged for 30 min at 3220 g and 15° C. Water and methanol plus 0.1% formic acid were used as mobile phase A and B, respectively. Samples were loaded with 20% mobile phase B at a flow rate of 0.2 mL/min and temperature of 45° C onto the analytical column (Kinetex C18 2.1x50mm, Phenomenex, California, USA). The flow was increased to 0.6 ml/min during the first 0.5 min of each run. In the same time, the introduced sample was inline diluted via a T-union with mobile phase A at a flow rate gradient of 0.4 to 0 mL x min^{-1} over 0.5 min. Afterwards, mobile phase B was linearly increased to 95% (0.5 to 2.5 min) and kept at this percentage for 1 minute. The system was reconditioned at 20% mobile B at the end of the run (3.5-4.0 min). Simvastatin acid and simvastatin acid-d6 eluted after 2.6 min. Both analytes were detected by electrospray ionization in the negative mode. The mass transition 435.3 → 318.8, 115.0 m/z and 441.2 → 319.2, 121.2 m/z were applied for simvastatin acid and simvastatin acid-d6 analysis, respectively. The following mass transition specific potentials were used: Declustering potential (DP) -105, collision energy (CE) -26 V, collision cell exit potential (CXP) -117 V for 435.3 → 318.8 m/z; DP of -105 V, CE -40 V, and a CXP of -5 V for 435.3 → 115.0 m/z; DP -110 V, CE -26 V, CXP -19 V for 441.2 →

319.2 m/z; DP -110 V, CE -44 V, CXP - 7 V for 441.2 → 121.2 m/z. The curtain gas was 10, collision gas was 4, ion sourced gas 1 was 60, ion source gas 2 was 50, ionspray voltage was -4200 V, entrance potential was -10 V, and the source temperature was 500 °C. The LC-MS/MS system was operated and data quantified using Analyst software 1.6.2 (AB Sciex, MA; USA).

4.4 Grip strength test

Grip strength, which is a validated parameter of muscle force [39], was measured on hind- and forelimbs using a grip strength test meter at days 1, 8, 14, and 22 over the treatment (Bioseb, Vitrolles, France). In order to measure their grip strength, the mouse was placed on the top of the grid and gently pulled by the tail down the grid using roughly the same pulling force and angle as the grid [39]. Each measurement was repeated 4 times in a succession of 5 seconds. Maximum peak grip force of both fore- and hindlimbs was measured. For each day grip strength was measured, it was normalized to body weight of that day. Subsequent grip strength measurements, during treatment, were compared to their initial grip strength at day 1 (set to 100%). All tests were performed blinded by the same operator.

4.5 Treadmill exercise

Mice were submitted to exhaustive exercise by incrementally increasing the speed on a treadmill (Treadmill Control, Panlab, Barcelona, Spain) with an electric grid. The electric grid, used to encourage the mice to run, delivered an electric shock with 0.4 mA current and 2 Hz frequency. This shock only causes an uncomfortable sensation but does not injure the mice. Mice were acclimatized to the apparatus for 2 consecutive days before the experiment. The acclimatization was performed as a 5-minute training at a speed of 17 cm/s and a slope of +10°. On the day of the experiment, a gas analyser was calibrated and the mice were placed in a hermetically sealed treadmill. Room air was pumped in and cage air was pumped out to the gas analyser. During the first 5 minutes, only room air and basal cage air with the mice were analysed by measuring oxygen consumption and carbon dioxide production. Afterwards, the treadmill session started at 17 cm/s for 5 minutes at a slope of +10°, followed by incremental increase of the speed by 2 cm/s every 2 minutes until exhaustion. Exhaustion was defined as continuous 5 seconds shock time due to inability of the mouse to run up the treadmill from the electric grid [40]. Blood lactate concentrations were determined in a sample collected from the tip of the tail before, and immediately after exercise using a lactate pro-LT device (Lactate Pro LT-1710, Arkray®, France). During the whole exercise session, the running distance and the number of shocks were determined. Oxygen consumption and carbon dioxide production were measured and used to calculate the respiratory exchange ratio (RER). RER is the ratio of the volume of carbon dioxide produced per minute divided by the volume of oxygen consumption over the same period of time. The RER is an indicator of substrate utilization: a RER at ≈0.7 indicates primarily oxidative of fatty acid, while a RER ≈1 represents primarily glucose metabolism [40]. Vertical mechanical work and power were calculated as previously described [40]. All tests were performed blinded by the same operator.

4.6 Sample collection

After 3 weeks of treatment, mice were anesthetized with an intraperitoneal injection of ketamine (160 mg/kg, Ketasol, Graeub, Bern, Switzerland) and xylazine (20 mg/kg, Rompun, Bayer, Leverkusen, Germany). Blood was removed from the apex of the heart and placed in a tube coated with EDTA. Plasma samples were obtained after centrifugation at 3000 rpm for 15 minutes at 4 °C. Tissues were immediately collected and weighed. A part of each muscle tissue was immediately frozen in isopentane cooled by liquid nitrogen and stored at -80 °C for later analysis and the remainder processed biochemical analysis. We conducted our experiments on different muscles, separating them by muscle type. Muscles are classified by mitochondrial mass: we used the superficial part of the gastrocnemius, and quadriceps muscle, which are mostly glycolytic (white), with a low mitochondrial content. For the oxidative-type muscles (red) with a high mitochondrial content, we studied the soleus muscle, the most oxidative red part of the gastrocnemius muscle located close to the soleus muscle, and the most oxidative red part of the quadriceps muscle located close to femur bone [31].

4.7 Mitochondrial respiration in permeabilized fibers

This technique ensured determination of global mitochondrial function, reflecting both the density as well as the functional properties of the muscle mitochondria. For this reason, we used saponin-skinned fibers, which kept mitochondria in their architectural environment, in superficial gastrocnemius, and soleus muscles as previously described [40,41]. Immediately after the sacrifice, the oxidative soleus muscle and the glycolytic superficial part of the gastrocnemius muscle were excised, cleaned of adipose and connective tissues under binocular microscope, and stored in ice cold Biops buffer containing 2.77 mM CaK_2-EGTA buffer, 7.23 mM K_2-EGTA, 5.77 mM Na_2ATP, 6.56 mM $MgCl_2$ ($6H_2O$), 20 mM taurine, 15 mM Na_2 Phosphocreatine, 20 mM imidazole, 0.5 mM dithiothreitol, and 50 mM MES hydrate, pH 7.1 at 4°C. Fibers were then washed for 30 min in Biops containing saponin (5 μg/mL) to permeabilize the fibers. To wash off excess saponin, fibers were washed two times for 5 minutes in the respiration medium (0.5 mM EGTA, 3 mM $MgCl_2$ ($6H_2O$), 20 mM taurine, 10 mM KH_2PO_4, 20 mM HEPES, 110 mM D-sucrose, 0.1 % bovine serum albumin, and 60 mM lactobionic acid; pH=7 at room temperature). Approximately 2-3 mg of fibers were placed in a thermostated oxygraphic chamber containing fresh respiration medium at 37°C with continuous stirring (Oxygraph-2k, Oroboros instruments, Innsbruck, Austria). After the determination of the basal oxygen consumption with glutamate (5 mM) and malate (2 mM), complex I substrate state was measured in the presence of saturating amount of adenosine diphosphate (2 mM ADP). The maximal OXPHOS respiration rate was then measured by adding succinate, as a substrate of complex II (25 mM). Complex I was then blocked with rotenone (0.5 μM), allowing to measure complex II-linked substrate state. Afterwards, complex II and complex III were inhibited by the injection of malonate (5 mM), and antimycin A (2.5 μM), respectively. Continuing the stepwise addition, cytochrome c (10 μM) was added to test for intactness of outer mitochondrial membrane. Complex IV-linked respiration was measured by adding N,N,N′,N′-tetramethyl-1,4-phenylendiamine (TMPD) (0.5 mM) and ascorbate (2 mM) and then inhibited with KCN (1 mM) as previously described [40]. Respiratory rates were expressed as pmol O_2 x s^{-1} x mg^{-1} wet weight.

4.8 Mitochondrial H_2O_2 production in permeabilized fibers

H_2O_2 production was studied from saponin-skinned fibers that keep mitochondria in their architectural environment, in superficial gastrocnemius, and soleus muscles. The permeabilized muscle bundles were placed in ice-cold buffer Z containing 110 mM K-methane sulfonate, 35 mM KCl, 1 mM EGTA, 5 mM K_2HPO_4, 3 mM $MgCl_2$, 6 mM H_2O, 0.05 mM glutamate, and 0.02 mM malate with 0.5 mg/ml BSA (pH 7.1, 295 mOsmol/kg H_2O). H_2O_2 production was measured with Amplex Red (Invitrogen Life Technologies, Rockville, MD, USA), which reacts with H_2O_2 in a 1:1 stoichiometry catalyzed by HRP (horseradish peroxidase; Invitrogen Life Technologies, Rockville, MD, USA) to yield the fluorescent compound resorufin and a molar equivalent of O_2 [42]. Resorufin has excitation and emission wavelengths of 563 nm and 587 nm, respectively, and is extremely stable once formed. Fluorescence was measured continuously with a Fluoromax 3 (Jobin Yvon) spectrofluorometer with temperature control and magnetic stirring. After a baseline (reactants only) had been established, the reaction was initiated by adding a permeabilized fiber bundle to 600 µL of buffer Z. Buffer Z contained 5 mM Amplex Red, 0.5 U/mL HRP, 5 mM glutamate, and 2 mM malate as substrates at 37°C. Succinate (25 mM) was then added for the measurement of H_2O_2 production under reverse electron flux condition. ADP (2mM) was added in order to determine C_{I+II}-linked substrate state H_2O_2 production for the determination of the Free Radical Leak (FRL). At the conclusion of each experiment, the H_2O_2 production rate was calculated from the background-subtracted slope of F/s, which was converted to concentration by using a standard curve (made with 1 nM H_2O_2 stepwise additions inside Z-buffer). H_2O_2 production rates were expressed as pmol x s^{-1} x mg^{-1} wet weight.

4.9 Free Radical Leak

H_2O_2 production and O_2 consumption were measured in parallel under similar experimental conditions (C_{I+II}-linked substrate state). This allowed the calculation of the fraction of electrons out of sequence, which reduce O_2 to ROS in the respiratory chain (the percentage of free radical leak) instead of reaching cytochrome oxidase to reduce O_2 to water [42]. Because two electrons are needed to reduce one mole of O_2 to H_2O_2, whereas four electrons are transferred in the reduction of one mole of O_2 to water, the percent of FRL was calculated as the rate of H_2O_2 production divided by twice the rate of O_2 consumption, and the result was multiplied by 100.

4.10 Quantitative Real Time Polymerase Chain Reaction (qRT-PCR)

Total RNA was obtained from superficial and the oxidative part of the gastrocnemius muscles using the RNeasy Fibrous Tissue Mini Kit (QIAGEN Gmbh, Hilden, Germany) according to the manufacturer's instructions. RNA was stored at −80°C until the reverse transcription reaction was performed. cDNA was synthetized from 1 µg total RNA with the Omniscript RT kit (QIAGEN Gmbh, Hilden, Germany). To perform the real-time PCR reaction, cDNA was mixed with each primer (sense and antisense (0.3 µM final concentration), SYBR Green (Roche Diagnostics, Mannheim, Germany) as a fluorescent dye and H_2O. The real-time PCR measurement of individual cDNAs was performed in triplicate using SYBR Green dye to measure duplex DNA formation with the ViiA™ 7 Real-

Time PCR System (Applied Biosystems, Waltham, MA, USA). The primer sequences were designed using information contained in the public database GenBank of the National Center for Biotechnology Information (NCBI). The sequences of the primer sets used are listed in Suppl. Table 2. Quantification of gene expression was performed by the method described in [43], using the *18s* gene as the internal control. The amplification efficiency of each sample was calculated as described by Ramakers et al. [44].

4.11 Total glutathione by LC/MS

10 mg of muscle tissue was homogenized with Mikro-Dismembrator (Mikro-Dismembrator S, Sartorius, Palaiseau, France) for 30 seconds at 2000 rpm. Tissue samples were solubilised and incubated on ice for 30 minutes with 25 μL per 10 mg tissue in a derivatization solution (containing 50 mM N-ethylmaleimide (NEM) dissolved in PBS (NEM-PBS)) to inhibit autoxidation of the GSH thiol group into GSSG. Methanol was added to the samples in a 1:4 ratio (v/v) to precipitate the protein. Samples were then centrifuged for 10 minutes at 4°C with 3500 rpm (Eppendorf 5415 R centrifuge, Germany). 250 μL of the supernatant was transferred into a new tube containing 250 μL of internal standard (IS, 400 nM GSSG-13C415N2 and 1μM GSH-d5-NEM dissolved in analytical grade water). Calibration lines of GSH-NEM (250 μM - 0.25 μM) and GSSG (25 μM - 0.025 μM) were prepared in the derivatization solution and diluted in methanol in a 1:4 ratio and mixed in a new tube with 250 μL of IS. Afterwards, 2.5 μL were injected into the LC–MS/MS system (Shimadzu HPLC, Kyoto, Japan, coupled to an API 4000 QTrap tandem mass spectrometer, ABSciex, Concord, Canada) to determine the GSH-NEM and GSSG levels in mouse skeletal muscle gastrocnemius. GSH-NEM and GSSG were separated on a Symmetry Polar C18 analytical column (3.5μM 4.6x75mm (WAT066224, Waters)) at 45 °C and a flow rate of 0.4 mL/min as previously described [45]. Water as a mobile phase A and acetonitrile as a mobile phase B were both supplemented with 0.1% acetic acid. Injected samples were then loaded into the analytical column by being inline diluted via a T union with mobile phase A during the first 0.5 min of each run. Afterwards, the gradient was increased linearly in the following 1.25 min, reaching 95% of mobile phase B. After each run, the column was washed for 0.5 min with 95% mobile phase B and washed again for another 0.75 min at 0% mobile phase B for reconditioning. The retention time of GSH-NEM was 1.8 min. The analytes GSH-NEM and GSSG were positively charged with ion spray voltage at 5500 eV and probe temperature was at 700 °C. Afterwards, they were analyzed with scheduled multiple reaction monitoring. The mass for GSH-NEM was at 433.1 → 304.0 m/z and for GSH-NEM-d5 was at 438.1 → 304.1 m/z. Total glutathione represents the sum of reduced GSH and oxidized GSSG.

4.12 Mitochondrial DNA (mtDNA) content

Approximately 5 mg of muscle tissue from white or red gastrocnemius was used for DNA extraction using the Nucleospin Tissue kit (Nucleospin Tissue, Macherey Nagel, Düren, Germany) as per manufacturer's instructions. Then, DNA samples were diluted to 10 ng/μL from which 1 μL was used for the quantitative real-time RT-PCR as described with some modifications [46]. To perform the real-time PCR reaction, diluted DNA was mixed with each primer (forward and reverse each containing 0.3 μM final concentration), SYBR Green (Roche Diagnostics, Mannheim, Germany) as a fluorescent dye and H_2O. The real-time PCR measurement of individual cDNAs was performed in triplicate using SYBR Green dye

to measure duplex DNA formation with the ViiA™ 7 Real-Time PCR System (Applied Biosystems, Waltham, MA, USA). Primer sequences used are shown in Suppl. Table 2. PCR run consisted of 40 cycles of amplification at 95°C for 15 seconds followed by 1 minute at 60°C. Relative amounts of nuclear and mitochondrial DNA were determined by comparison of amplification kinetics of Hexokinase 2 (*Hk2*) and *Cox2* as described by [47]. mtDNA content was assessed by calculating the inverse of the CT_{Cox2}/CT_{Hk2} ratio [27].

4.13 Citrate synthase (CS) activity

Pieces of frozen muscle (5–10 mg wet weight) were homogenized with a vibrating microbead homogenizer (Mikro-Dismembrator, Sartorius®, Palaiseau, France) in a ratio (W/V) of 1/20 with a buffer containing 5 mM HEPES, 1 mM EGTA and 1 mM DTT, pH 8.7. The homogenate was then supplemented with 0.1% Triton X-100 and incubated on ice for 1 h. After centrifugation for 5 min at 3000 rpm, CS activity was determined in the supernatant by spectrophotometry (Tecan M200 Pro Infinity plate reader, Männedorf, Switzerland) using a 96-well plate as described by Srere [48]. Values were reported as nmol x min^{-1} x mg^{-1} of dry tissue weight.

4.14 Electron transmission microscopy and analysis of the mitochondrial number and size

A portion of freshly excised muscle (quadriceps femoris) was cut as 0.5 x 0.2 x 0.2 cm strip and fixed overnight at 4 °C with 2.5% glutaraldehyde and 2% paraformaldehyde in PIPES buffer (0.1 M at pH 7). Afterwards, the sample is washed three times with 0.1 M PIPES buffer at pH 7 and postfixed in 1% buffered osmium tetroxide for 1h at 4 °C. Then, the sample was rinsed in distilled water and placed in an "en bloc" and stained with aqueous uranyl acetate for 1h at 4 °C in the dark. Cubes were then dehydrated in an ethanol series (30%, 50%, 75%, 95%, and 100%). The dehydrated samples were washed in acetone and finally embedded in Epon 812 resin.

Embedding was carried out in an 60°C oven for 48h until the epoxy resin was completely hardened and ready for sectioning. Ultrathin sections were cut with a diamond knife and placed on copper grids coated with Parlodion film and carbon layer impregnated with uranyl acetate and lead citrate. Sections were analyzed using a FEI Tecnai T12 transmission electron microscope operating at 12 kV. Images were recorded using a TVIPS F416 CMOS digital camera. For the quantitative analysis of EM micrographs, non-overlapping 64 μm^2 regions were randomly taken from transversal sections of the internal part of the quadriceps. Mitochondria were manually outlined on the micrographs using the Fiji software [49].

4.15 Statistical analysis

Data are represented as means ± SEM. Statistical analyses were performed using unpaired *t* tests (comparison of 2 unrelated means) or 2-way ANOVA followed by a Bonferroni's post-test for the comparison of multiple means using GraphPad Prism 8 (Graph Pad Software, Inc., San Diego, CA, USA). Significance was set at $p < 0.05$.

Supplementary Material

Refer to Web version on PubMed Central for supplementary material.

Acknowledgements

References

1. Taylor FC, Huffman M, Ebrahim S. Statin therapy for primary prevention of cardiovascular disease. JAMA. 2013; 310(22):2451–2452. [PubMed: 24276813]

2. Staffa JA, Chang J, Green L. Cerivastatin and reports of fatal rhabdomyolysis. N Engl J Med. 2002; 346(7):539–540.

3. Schirris TJ, Renkema GH, Ritschel T, et al. Statin-Induced Myopathy Is Associated with Mitochondrial Complex III Inhibition. Cell Metab. 2015; 22(3):399–407. [PubMed: 26331605]

4. Bouitbir J, Sanvee GM, Panajatovic MV, Singh F, Krahenbuhl S. Mechanisms of statin-associated skeletal muscle-associated symptoms. Pharmacol Res. 2019

5. Evans M, Rees A. Effects of HMG-CoA reductase inhibitors on skeletal muscle: are all statins the same? Drug Saf. 2002; 25(9):649–663. [PubMed: 12137559]

6. Banach M, Serban C, Sahebkar A, et al. Effects of coenzyme Q10 on statin-induced myopathy: a meta-analysis of randomized controlled trials. Mayo Clinic proceedings. 2015; 90(1):24–34. [PubMed: 25440725]

7. Kaufmann P, Torok M, Zahno A, Waldhauser KM, Brecht K, Krahenbuhl S. Toxicity of statins on rat skeletal muscle mitochondria. Cellular and Molecular Life Sciences. 2006; 63(19-20):2415–2425. [PubMed: 17013560]

8. Sirvent P, Mercier J, Lacampagne A. New insights into mechanisms of statin-associated myotoxicity. Curr Opin Pharmacol. 2008; 8(3):333–338. [PubMed: 18243052]

9. Bouitbir J, Charles AL, Rasseneur L, et al. Atorvastatin treatment reduces exercise capacities in rats: involvement of mitochondrial impairments and oxidative stress. J Appl Physiol. 2011; 111(5):1477–1483. [PubMed: 21852406]

10. Brookes PS. Mitochondrial H(+) leak and ROS generation: an odd couple. Free Radic Biol Med. 2005; 38(1):12–23. [PubMed: 15589367]

11. Piantadosi CA, Carraway MS, Babiker A, Suliman HB. Heme oxygenase-1 regulates cardiac mitochondrial biogenesis via Nrf2-mediated transcriptional control of nuclear respiratory factor-1. Circ Res. 2008; 103(11):1232–1240. [PubMed: 18845810]

12. Lecarpentier Y. Physiological role of free radicals in skeletal muscles. J Appl Physiol. 2007; 103(6):1917–1918. [PubMed: 17916668]

13. Sano M, Fukuda K. Activation of mitochondrial biogenesis by hormesis. Circ Res. 2008; 103(11):1191–1193. [PubMed: 19028915]

14. Robinson MM, Hamilton KL, Miller BF. The interactions of some commonly consumed drugs with mitochondrial adaptations to exercise. J Appl Physiol. 2009; 107(1):8–16. [PubMed: 19423832]

15. Bouitbir J, Charles AL, Echaniz-Laguna A, et al. Opposite effects of statins on mitochondria of cardiac and skeletal muscles: a 'mitohormesis' mechanism involving reactive oxygen species and PGC-1. Eur Heart J. 2012; 33(11):1397–1407. [PubMed: 21775390]

16. Handschin C, Chin S, Li P, et al. Skeletal muscle fiber-type switching, exercise intolerance, and myopathy in PGC-1alpha muscle-specific knock-out animals. J Biol Chem. 2007; 282(41):30014–30021. [PubMed: 17702743]

17. Perez-Schindler J, Svensson K, Vargas-Fernandez E, Santos G, Wahli W, Handschin C. The coactivator PGC-1alpha regulates skeletal muscle oxidative metabolism independently of the nuclear receptor PPARbeta/delta in sedentary mice fed a regular chow diet. Diabetologia. 2014; 57(11):2405–2412. [PubMed: 25116175]

18. Bjorkhem-Bergman L, Lindh JD, Bergman P. What is a relevant statin concentration in cell experiments claiming pleiotropic effects? Br J Clin Pharmacol. 2011; 72(1):164–165. [PubMed: 21223360]

19. Balaban RS, Nemoto S, Finkel T. Mitochondria, oxidants, and aging. Cell. 2005; 120(4):483–495. [PubMed: 15734681]

20. Wang Y, Branicky R, Noe A, Hekimi S. Superoxide dismutases: Dual roles in controlling ROS damage and regulating ROS signaling. J Cell Biol. 2018; 217(6):1915–1928. [PubMed: 29669742]

21. Felser A, Blum K, Lindinger PW, Bouitbir J, Krahenbuhl S. Mechanisms of hepatocellular toxicity associated with dronedarone--a comparison to amiodarone. Toxicol Sci. 2013; 131(2):480–490. [PubMed: 23135547]

22. Larsen S, Nielsen J, Hansen CN, et al. Biomarkers of mitochondrial content in skeletal muscle of healthy young human subjects. J Physiol. 2012; 590(14):3349–3360. [PubMed: 22586215]

23. Reagan-Shaw S, Nihal M, Ahmad N. Dose translation from animal to human studies revisited. FASEB journal : official publication of the Federation of American Societies for Experimental Biology. 2008; 22(3):659–661. [PubMed: 17942826]

24. Bonifacio A, Mullen PJ, Mityko IS, Navegantes LC, Bouitbir J, Krahenbuhl S. Simvastatin induces mitochondrial dysfunction and increased atrogin-1 expression in H9c2 cardiomyocytes and mice in vivo. Arch Toxicol. 2016; 90(1):203–215. [PubMed: 25300705]

25. Bonifacio A, Sanvee GM, Bouitbir J, Krahenbuhl S. The AKT/mTOR signaling pathway plays a key role in statin-induced myotoxicity. Biochim Biophys Acta. 2015; 1853(8):1841–1849. [PubMed: 25913013]

26. Bonifacio A, Sanvee GM, Brecht K, et al. IGF-1 prevents simvastatin-induced myotoxicity in C2C12 myotubes. Arch Toxicol. 2017; 91(5):2223–2234. [PubMed: 27734117]

27. Singh F, Zoll J, Duthaler U, et al. PGC-1beta modulates statin-associated myotoxicity in mice. Arch Toxicol. 2019; 93(2):487–504. [PubMed: 30511338]

28. Kwak HB, Thalacker-Mercer A, Anderson EJ, et al. Simvastatin impairs ADP-stimulated respiration and increases mitochondrial oxidative stress in primary human skeletal myotubes. Free radical biology & medicine. 2012; 52(1):198–207. [PubMed: 22080086]

29. Paiva H, Thelen KM, Van Coster R, et al. High-dose statins and skeletal muscle metabolism in humans: a randomized, controlled trial. Clinical pharmacology and therapeutics. 2005; 78(1):60–68. [PubMed: 16003294]

30. Lenaz G. The mitochondrial production of reactive oxygen species: mechanisms and implications in human pathology. IUBMB Life. 2001; 52(3–5):159–164. [PubMed: 11798028]

31. Bouitbir J, Singh F, Charles AL, et al. Statins Trigger Mitochondrial Reactive Oxygen Species-Induced Apoptosis in Glycolytic Skeletal Muscle. Antioxid Redox Signal. 2016; 24(2):84–98. [PubMed: 26414931]

32. Musatov A, Robinson NC. Susceptibility of mitochondrial electron-transport complexes to oxidative damage. Focus on cytochrome c oxidase. Free radical research. 2012; 46(11):1313–1326. [PubMed: 22856385]

33. Finck BN, Kelly DP. PGC-1 coactivators: inducible regulators of energy metabolism in health and disease. The Journal of clinical investigation. 2006; 116(3):615–622. [PubMed: 16511594]

34. Leone TC, Lehman JJ, Finck BN, et al. PGC-1alpha deficiency causes multi-system energy metabolic derangements: muscle dysfunction, abnormal weight control and hepatic steatosis. PLoS biology. 2005; 3(4):e101. [PubMed: 15760270]

35. Lin J, Wu H, Tarr PT, et al. Transcriptional co-activator PGC-1 alpha drives the formation of slow-twitch muscle fibres. Nature. 2002; 418(6899):797–801. [PubMed: 12181572]

36. Handschin C, Choi CS, Chin S, et al. Abnormal glucose homeostasis in skeletal muscle-specific PGC-1alpha knockout mice reveals skeletal muscle-pancreatic beta cell crosstalk. J Clin Invest. 2007; 117(11):3463–3474. [PubMed: 17932564]

37. Handschin C, Spiegelman BM. Peroxisome proliferator-activated receptor gamma coactivator 1 coactivators, energy homeostasis, and metabolism. Endocr Rev. 2006; 27(7):728–735. [PubMed: 17018837]

38. Higgins JW, Bao JQ, Ke AB, et al. Utility of Oatp1a/1b-knockout and OATP1B1/3-humanized mice in the study of OATP-mediated pharmacokinetics and tissue distribution: case studies with pravastatin, atorvastatin, simvastatin, and carboxydichlorofluorescein. Drug Metab Dispos. 2014; 42(1):182–192. [PubMed: 24194513]

39. Capers PL, Hyacinth HI, Cue S, et al. Body composition and grip strength are improved in transgenic sickle mice fed a high-protein diet. J Nutr Sci. 2015; 4:e6. [PubMed: 26090102]

40. Bouitbir J, Haegler P, Singh F, et al. Impaired Exercise Performance and Skeletal Muscle Mitochondrial Function in Rats with Secondary Carnitine Deficiency. Front Physiol. 2016; 7:345. [PubMed: 27559315]

41. Kuznetsov AV, Veksler V, Gellerich FN, Saks V, Margreiter R, Kunz WS. Analysis of mitochondrial function in situ in permeabilized muscle fibers, tissues and cells. Nat Protoc. 2008; 3(6):965–976. [PubMed: 18536644]

42. Anderson EJ, Neufer PD. Type II skeletal myofibers possess unique properties that potentiate mitochondrial H(2)O(2) generation. Am J Physiol Cell Physiol. 2006; 290(3):C844–851. [PubMed: 16251473]

43. Liu W, Saint DA. Validation of a quantitative method for real time PCR kinetics. Biochem Biophys Res Commun. 2002; 294(2):347–353. [PubMed: 12051718]

44. Ramakers C, Ruijter JM, Deprez RH, Moorman AF. Assumption-free analysis of quantitative real-time polymerase chain reaction (PCR) data. Neurosci Lett. 2003; 339(1):62–66. [PubMed: 12618301]

45. Paech F, Abegg VF, Duthaler U, Terracciano L, Bouitbir J, Krahenbuhl S. Sunitinib induces hepatocyte mitochondrial damage and apoptosis in mice. Toxicology. 2018; 409:13–23. [PubMed: 30031043]

46. Pieters N, Koppen G, Smeets K, et al. Decreased mitochondrial DNA content in association with exposure to polycyclic aromatic hydrocarbons in house dust during wintertime: from a population enquiry to cell culture. PLoS One. 2013; 8(5):e63208. [PubMed: 23658810]

47. Gariani K, Menzies KJ, Ryu D, et al. Eliciting the mitochondrial unfolded protein response by nicotinamide adenine dinucleotide repletion reverses fatty liver disease in mice. Hepatology. 2016; 63(4):1190–1204. [PubMed: 26404765]

48. Srere PA. [1] Citrate synthase. 1969; 13:3–11.

49. Leduc-Gaudet JP, Picard M, St-Jean Pelletier F, et al. Mitochondrial morphology is altered in atrophied skeletal muscle of aged mice. Oncotarget. 2015; 6(20):17923–17937. [PubMed: 26053100]
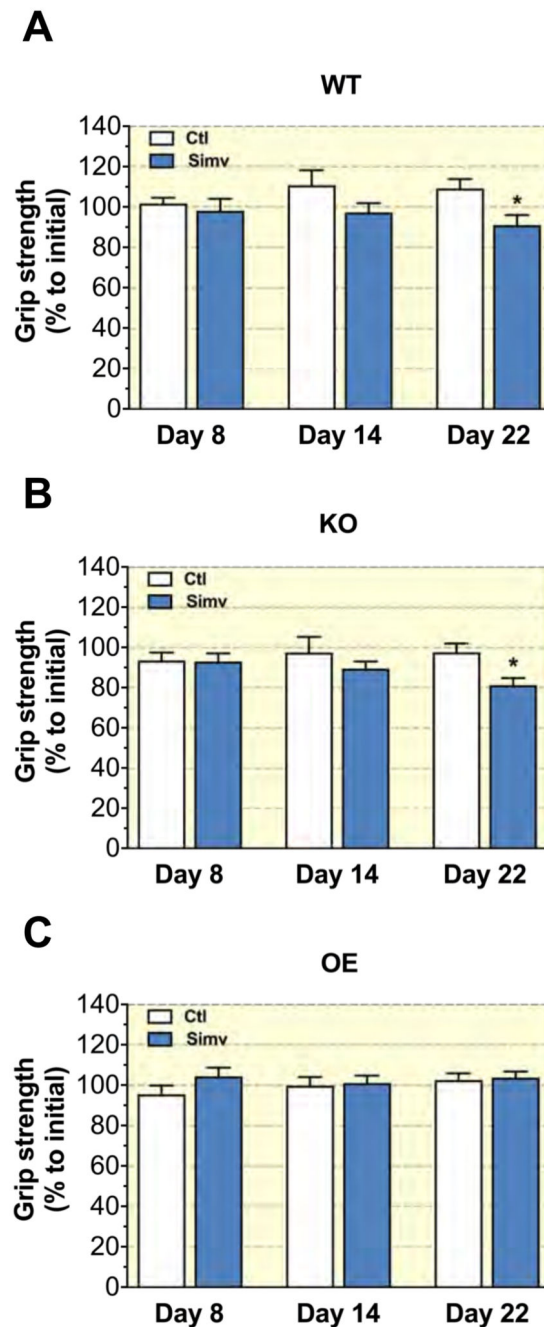
Figure 1. Grip strength.
The grip strength was determined on hind- and forelimbs using a grip strength test meter at days 1, 8, 14, and 22 of the treatment period in **(A)** WT, **(B)** KO and **(C)** OE mice. The value at day 1 of each treatment group was set at 100%. The operator was blinded regarding the treatment of the mice. Data were normalized to body weight and are represented as mean ± SEM of 10 animals per group. *p < 0.05 between simvastatin treated and the respective control group. Abbreviations: WT, wild type; KO, PGC-1α knock-out mice; OE, PGC-1α overexpressing mice; Ctl: control; Simv, simvastatin.
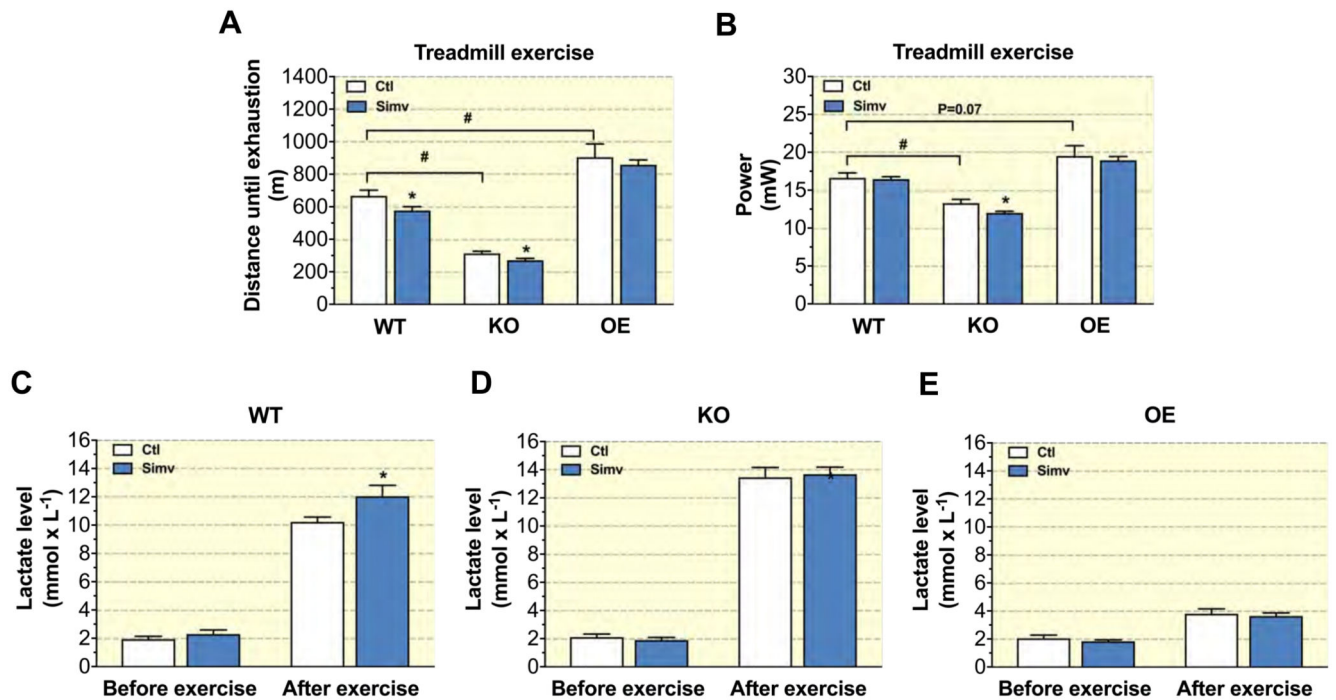
Figure 2. Physical capacity.
Physical capacity was determined using a treadmill as **(A)** distance until exhaustion and as **(B)** vertical mechanical power in mice treated or not with simvastatin for 3 weeks for each mouse model. Blood lactate was determined before and after exhaustive treadmill exercise in **(C)** WT, **(D)** KO and **(E)** OE mice. Data are presented as mean ± SEM of 10 animals per group. *p < 0.05 between simvastatin-treated and respective control mice. #p < 0.05 between control groups of WT, KO and OE mice. Abbreviations: WT, wild type; KO, PGC-1α knock-out mice; OE, PGC-1α overexpressing mice; Ctl: control; Simv, simvastatin.
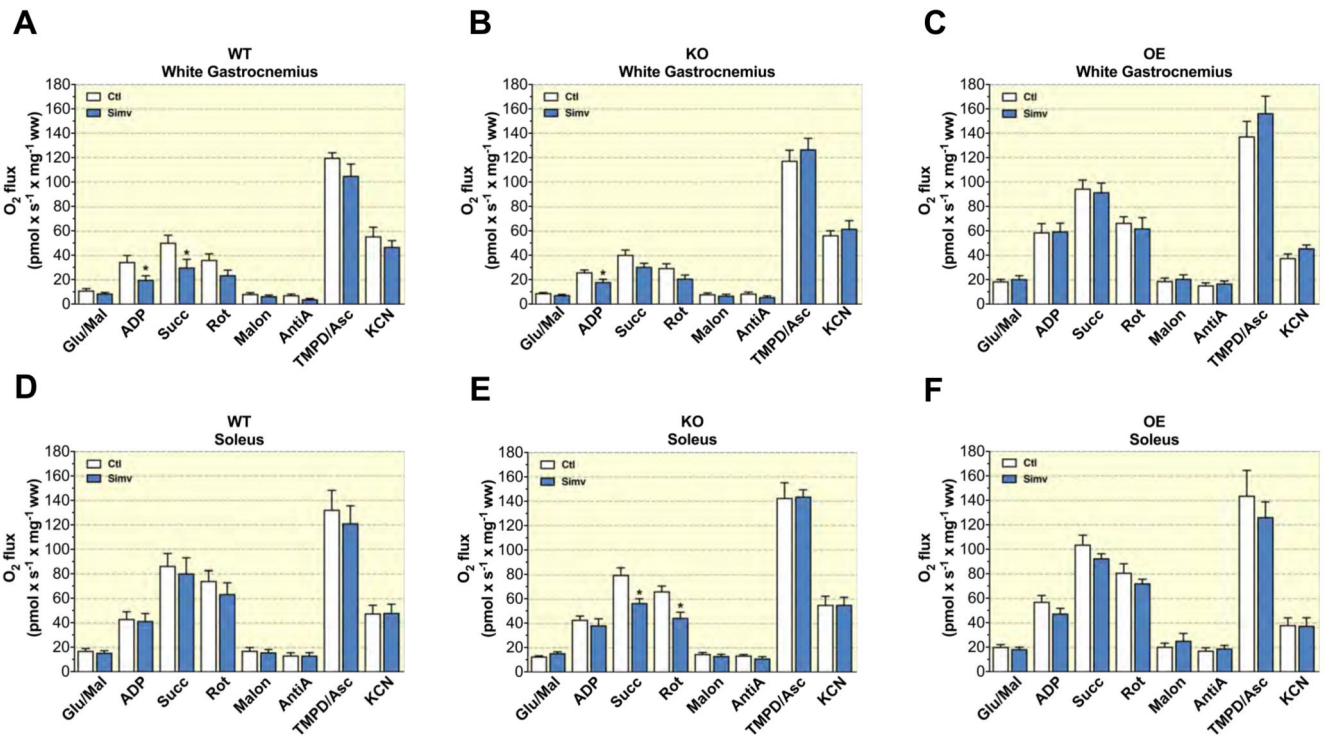
Figure 3. Mitochondrial respiration by permeabilized muscle fibres.
Mitochondrial respiratory capacity was measured in saponin permeabilized muscle fibres
with complex I-, II- and IV-linked substrates and their respective inhibitors for glycolytic
muscle (white part of gastrocnemius) in **(A)** WT, **(B)** KO, and **(C)** OE and for oxidative
muscle (soleus) in **(D)** WT, **(E)** KO, and **(F)** OE mice. Data are represented as mean ± SEM
of 10 animals per group. *p <0.05 between simvastatin-treated and respective control mice.
Abbreviations: WT, wild type; KO, PGC-1α knock-out mice; OE, PGC-1α overexpressing
mice; Glu/Mal, glutamate/malate; Succ, succinate; Rot, rotenone; Malon, malonate; AntiA,
antimycin A; TMPD/Asc, N,N,N′,N′-tetramethyl-1,4-phenylendiamine/ascorbate; Ctl:
control; Simv, simvastatin; ww, wet weight.
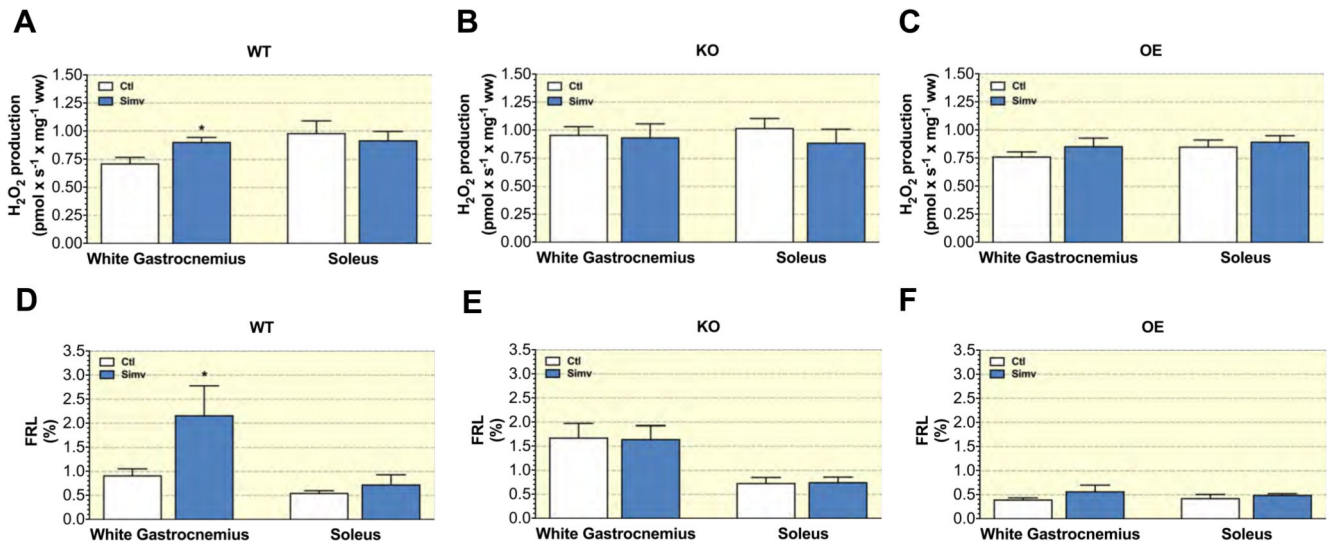
Figure 4. Mitochondrial H$_2$O$_2$ production in permeabilized muscle fibres.
Mitochondrial H$_2$O$_2$ production by superficial gastrocnemius muscle, and soleus muscle of **(A)** WT, **(B)** KO, and **(C)** OE mice. Mitochondrial free radical leak for white gastrocnemius muscle, and soleus muscle of **(D)** WT, **(E)** KO, and **(F)** OE mice. Data are represented as mean ± SEM of 10 animals per group. *p < 0.05 simvastatin-treated and respective control groups. Abbreviations: WT, wild type; KO, PGC-1α knock-out mice; OE, PGC-1α overexpressing mice; Ctl: control; Simv, simvastatin; ww, wet weight.
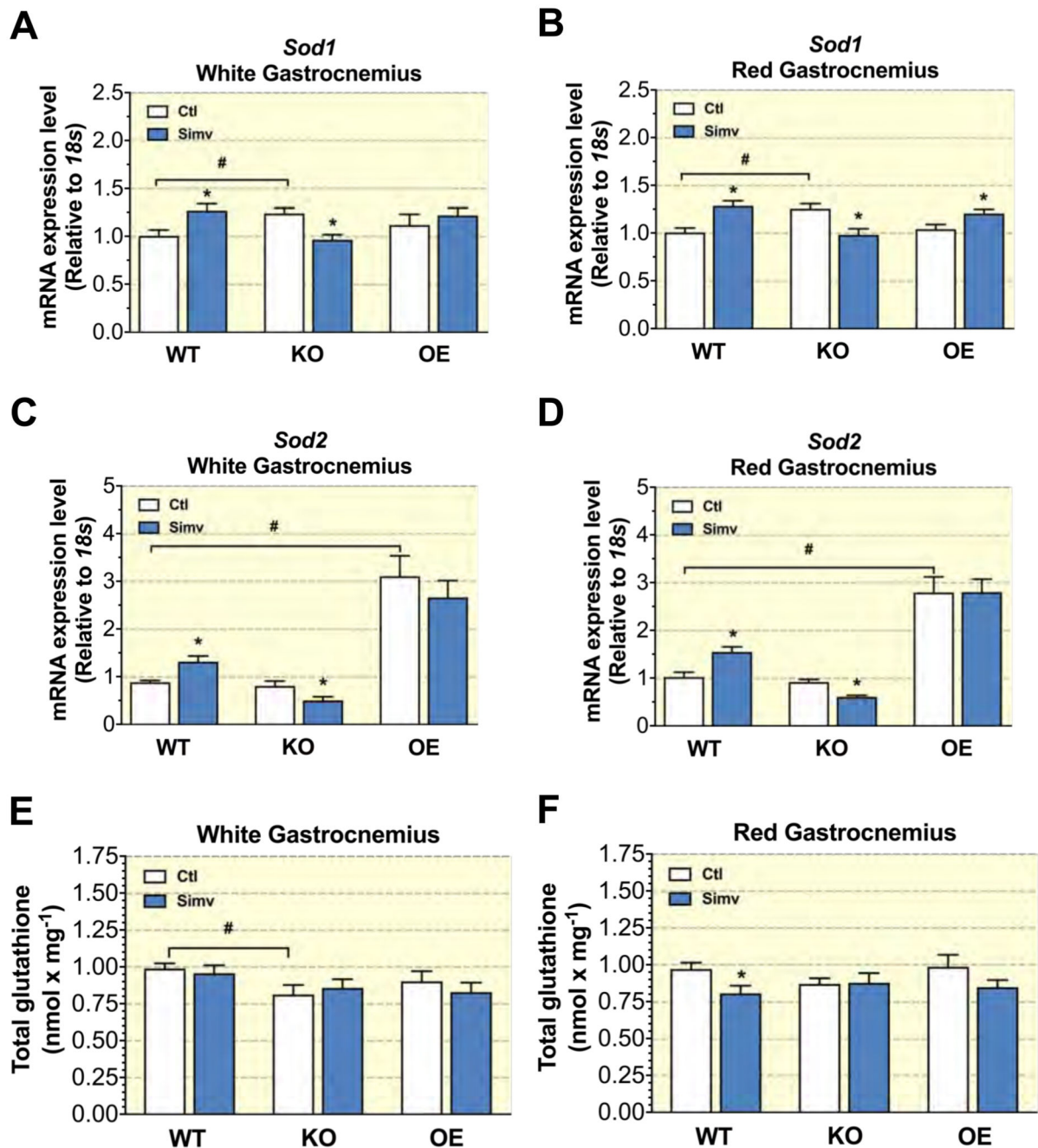
**Figure 5. Antioxidative defense in skeletal muscles.**
Sod1 and *Sod2* mRNA expression in the white (**A** and **C**, respectively) and red (**B** and **D**, respectively) part of gastrocnemius. Muscle content of total glutathione for the white (**E**) and red (**F**) part of gastrocnemius. Data are presented as mean ± SEM of 10 animals per group. *p <0.05 between simvastatin-treated and control mice. #p < 0.05 between control groups of WT, KO and OE mice. Abbreviations: WT, wild type; KO, PGC-1α knock-out mice; OE, PGC-1α overexpressing mice; Ctl: control; Simv, simvastatin.
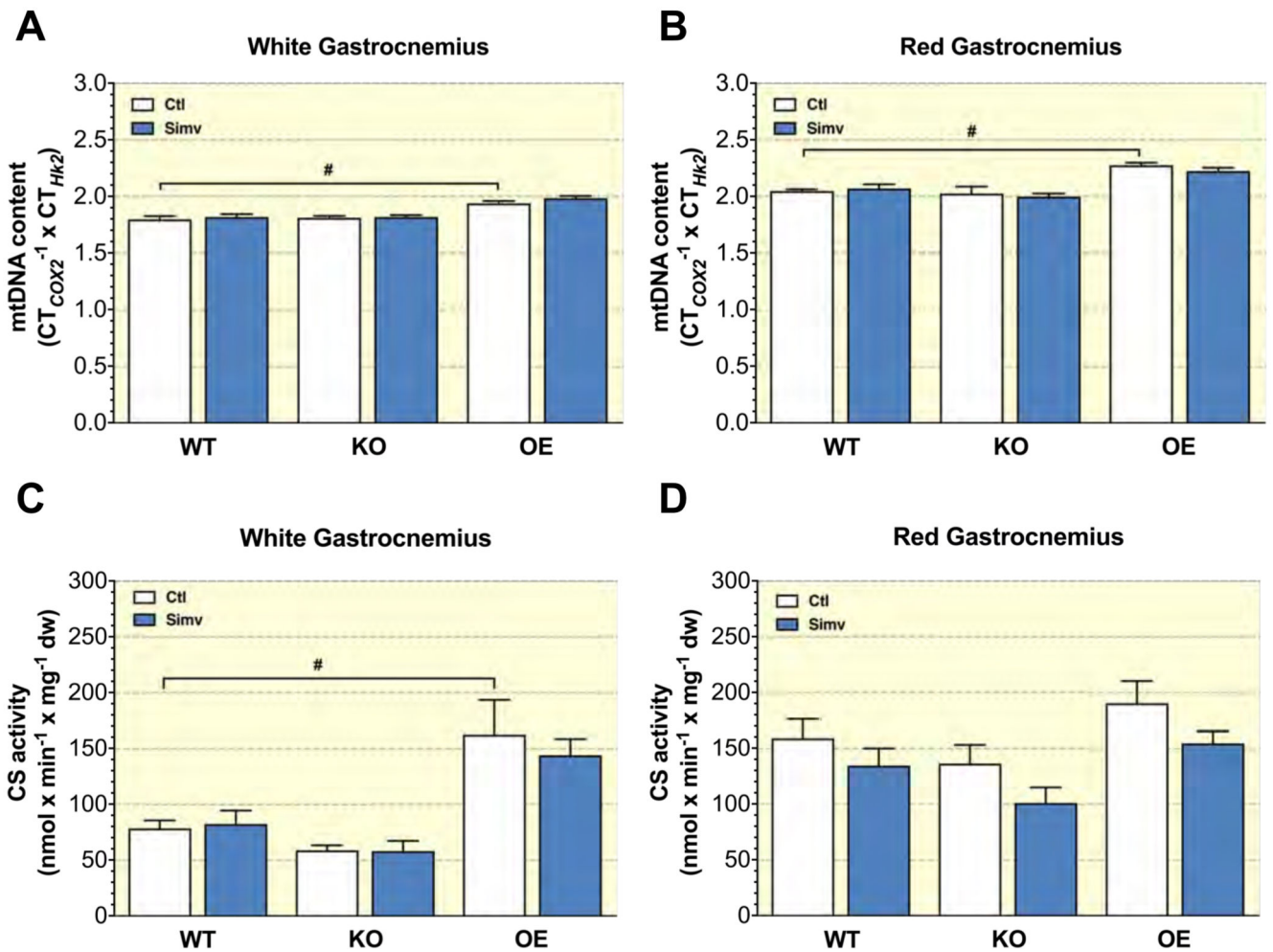
Figure 6. Mitochondrial DNA content and citrate synthase activity in skeletal muscle.
Mitochondrial DNA quantification in the **(A)** white part of gastrocnemius and **(B)** in the red part of gastrocnemius. Citrate synthase activity is shown for the white **(C)** and the red **(D)** part of gastrocnemius normalized to mg tissue weight. Data are presented as mean ± SEM of 10 animals per group. *p <0.05 between simvastatin-treated and control mice. #p <0.05 the control groups of KO or OE mice and WT mice. Abbreviations: WT, wild type; KO, PGC-1α knock-out mice; OE, PGC-1α overexpressing mice; Ctl: control; Simv, simvastatin; dw, dry weight.
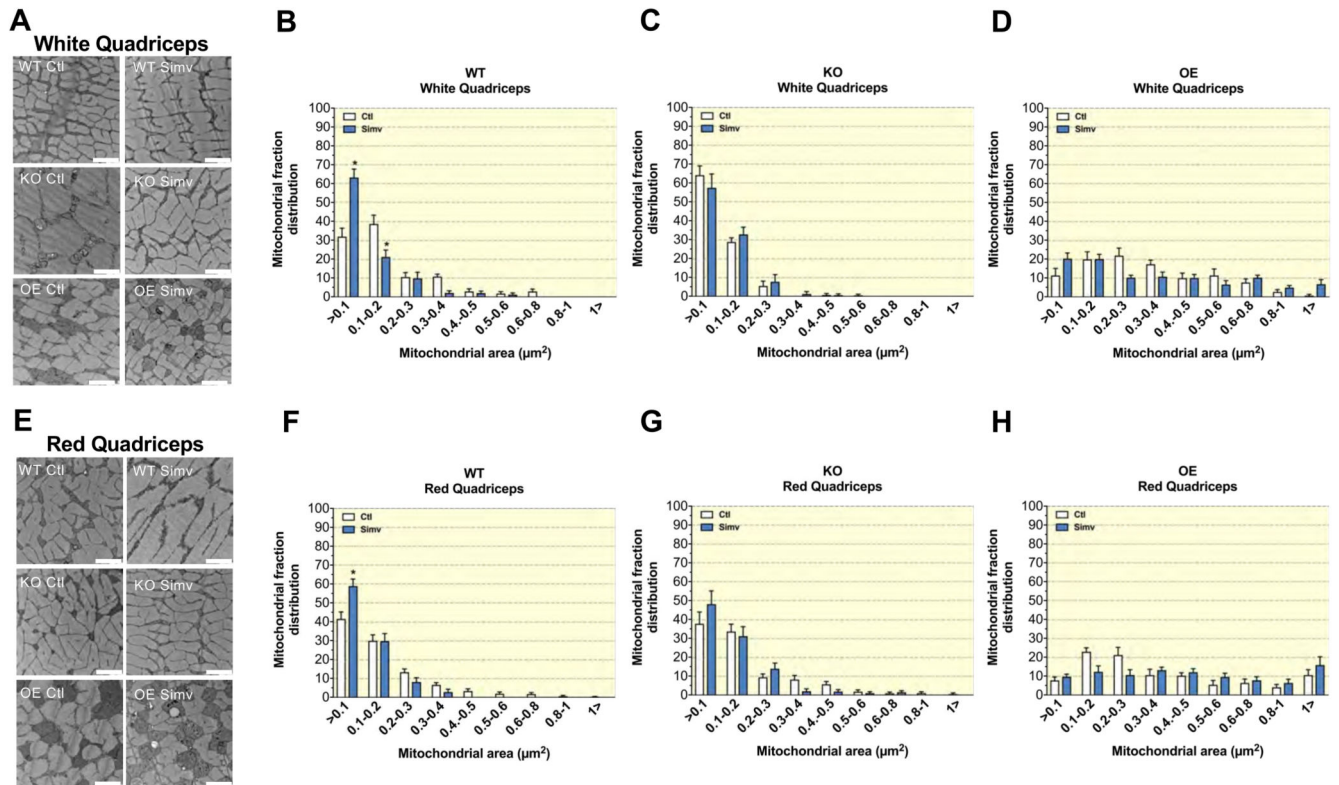
Figure 7. Mitochondrial cross-section area distribution.

Representative electron microscopy micrographs for all treatment groups showing sections of white (**A**) and red (**E**) quadriceps. The frequency distribution of the mitochondrial cross-section area is shown for the white quadriceps (WQ) in (**B**) WT, (**C**) KO, and (**D**) OE mice, and for the red quadriceps (RQ) in (**F**) WT, (**G**) KO, and (**H**) OE mice. Data are presented as mean ± SEM of 6 separate micrographs per group. The white bar in each picture represents 2 μm. Abbreviations: WT, wild type; KO, PGC-1α knock-out mice; OE, PGC-1α overexpressing mice; Ctl: control; Simv, simvastatin.

Table 1

Characterization of control (Ctl) and simvastatin-treated (Simv) mice.

Mouse model	WT		KO		OE	
Treatment	Ctl	Simv	Ctl	Simv	Ctl	Simv
Physiological parameter						
End study body weight (g)	29.3±0.5	29.8±0.8	29.9±0.9	29.0±0.8	28.1±1.0	28.8±0.9
Daily food intake (g)	3.64±0.17	3.67±0.21	3.70±0.14	3.95±0.1	3.56±0.15	3.48±0.08
Daily water intake (mL)	4.45±0.25	4.42±0.33	4.46±0.16	4.54±0.2	4.17±0.25	4.38±0.12
Organ weight (weight per femur length in g x mm^{-1})						
Heart	7.82±0.48	7.46±0.52	7.21±0.44	7.12±0.21	7.42±0.45	7.48±0.21
Gastrocnemius	9.08±0.35	9.26±0.39	9.70±0.41	10.28±0.39	9.08±0.36	9.51±0.36
Soleus	0.44±0.01	0.53±0.01 [*]	0.45±0.03	0.53±0.03	0.53±0.04 [#]	0.51±0.05
EDL	4.11±0.21	4.32±0.14	4.17±0.24	4.36±0.26	4.26±0.06	4.28±0.33
Quadriceps	12.9±0.7	13.5±0.6	12.2±0.9	11.9±0.3	10.8±0.5 [#]	11.5±0.5

WT wild-type mice; KO, muscle PGC-1α knockout mice; OE, muscle PGC-1α overexpression mice; EDL, extensor digitorum longus. All values are expressed as mean±SEM with n=10 per group.

[*] p<0.05 between simvastatin-treated and control mice

[#] p<0.05 between the control groups of KO or OE mice and WT mice.